

KATARZYNA TKACZ-ŚMIECH, MAREK DANIELEWSKI, BOGUSIAW BOŻEK,
KATARZYNA BERENT, DARIUSZ ZIENTARA, and MAREK ZAJUSZ

In high-temperature coatings, welded parts, and a range of other applications, components in the contact zone interdiffuse at elevated temperatures and may react to change the phase composition. The diffusion zone can be complex and can consist of sequential layers of intermediate phases, solid solutions, and in the case of multicomponent systems also of multiphase layers. In this work, the interdiffusion in Ni-Cr-Al alloys is studied experimentally and modeled numerically. The diffusion multiples were prepared by hot isostatic pressing and post-annealing at 1473 K (1200 °C). The concentration profiles were measured with wide-line EDS technique which allowed obtaining high-accuracy diffusion paths. The experimental profiles and diffusion paths were compared with numerical results simulated with application of very recent model of interdiffusion in multicomponent–multiphase systems. The calculated and experimental data show good agreement.

DOI: 10.1007/s11661-017-4051-8

© The Author(s) 2017. This article is published with open access at Springerlink.com

I. INTRODUCTION

THE interdiffusion in multicomponent systems controls many technological processes, such as nitriding, carburizing, and aluminizing. It can, however, also appear as negative phenomenon, causing degradation of protective coatings and alloys. A problem is that diffusion in multicomponent systems can be followed by a formation of multiphase zones of complex morphologies. Such zones can grow in ternary and more component systems which are allowed by Gibbs phase rule.

The diffusion in two- and multiphase zones differs from the diffusion in the single phase and can lead to the effects such as zigzag diffusion, horns at the diffusion path, and jumps of the concentrations without typical interphase boundary.^[1,2]

In this work, we study diffusion between single- and two-phase Ni-Cr-Al alloys. The alloys from this system are a basis for the development of numerous creep-resistant alloys. The interest in this system is prompted by the applications of nickel-based superalloys in gas turbines and jet engines working at high temperatures. These alloys have superior mechanical properties and high heat resistance at high temperatures.^[3]

The importance of the Ni-Cr-Al system is followed by numerous experimental and theoretical studies of the phase diagrams for this system.^[4–19] Most of the

research is confined to Ni-rich corner at high temperatures, *i.e.*, above 1273 K (1000 °C).

Due to experimental difficulties, the bibliography dedicated to diffusion in Ni-Cr-Al alloys is limited, and there are only few experimental results.^[20–27] Over forty Ni-Cr-Al diffusion couples, in $\gamma|\gamma + \beta$ multiphase couples, were experimentally studied by Nesbitt and Heckel.^[26] The samples were annealed at 1373 K and 1473 K (1100 °C and 1200 °C) for 100 hours, and the concentration profiles and diffusion paths measured. The measurement was made in γ phase only. The concentrations and diffusion path in two-phase zone were approximated from the terminal compositions.

As follows in Reference 22 experimental and simulated results of simulations of interdiffusion in $\gamma + \beta|\gamma$ couple were presented. The agreement between calculated and measured diffusion paths was, however, very weak. In Reference 28, DICTRA software was applied and interdiffusion in $\gamma + \beta|\gamma$ simulated. The simulated and measured diffusion paths remained in good agreement. The authors revealed the recession of two-phase zone which agreed with experiment. Unfortunately, the authors have not revealed the kinetic coefficients used in the calculations.

This work shows the progress in the field of mass transport in multiphase systems. It is our aim to combine new experimental technique with advanced modeling of interdiffusion, determinate diffusion profiles and paths, and to characterize the phenomena that follow diffusion in the studied system.

In particular, the diffusion multiple method^[29] and the wide-line EDS analysis (WL-EDS)^[30] in combined with Savitzky-Golay filtering^[31] are applied to obtain high-quality experimental diffusion profiles. The experimental data are compared with the results simulated with application of our very recent phenomenological model of interdiffusion in the two-phase zone.^[32]

KATARZYNA TKACZ-ŚMIECH, MAREK DANIELEWSKI, DARIUSZ ZIENTARA, and MAREK ZAJUSZ are with the Faculty of Materials Science and Ceramics, AGH University of Science and Technology, 30-059 Kraków, Poland. BOGUSIAW BOŻEK is with the Faculty of Applied Mathematics, AGH University of Science and Technology, 30-059 Kraków, Poland. KATARZYNA BERENT is with the ACMiN, AGH University of Science and Technology, 30-059 Kraków, Poland. Contact e-mail: zajuszm@agh.edu.pl

Manuscript submitted August 26, 2016.

Article published online March 9, 2017

II. SAMPLE PREPARATION

To study experimentally the interdiffusion in Ni-Cr-Al system, the diffusion multiple method developed by Zhao in 2001^[29] is used. The method allows obtaining a large number of data from single experiment and can be used to investigate phase diagrams, precipitate-growth kinetics, and interdiffusion.^[29,33–36]

Four alloys, as specified in Table I, were used to produce diffusion multiple. The alloys' rods were cut into bars 20-mm long and into the 1/4 sections and then polished. Prepared bars were placed in the cylindrical container made of the 200/201 nickel alloy with nickel content 99.0 pct. The external diameter of the container was 16 mm, internal—10 mm. The schema of the multiple is shown in Figure 1.

The container with the samples was vacuum welded with electron beam under the pressure 2×10^{-5} mbar and then subjected to 1-hour hot isostatic pressing (HIP) at 1473 K (1200 °C), under the pressure 200 MPa. The sample was cooled inside the furnace. Then, it was cut into slices about 3-mm thick, which were abraded to remove cut-offs. Chosen samples were subjected to further annealing in vacuum-closed quartz ampoule. Annealing was conducted in the furnace chamber, for 25 hours at 1473 ± 5 K (1200 ± 5 °C). After this time, it was water quenched and then subjected to further examination.

To eliminate an impact of surface effects on diffusion profiles, the samples were grounded and about 1-mm-thick layer of the material was removed. Next, they were polished by $0.25 \mu\text{m}$ SiO₂ suspension. After the process, the samples were about 1-mm thick.

III. CONCENTRATION PROFILE MEASUREMENTS

SEM micrographs and EDS analysis of concentration profiles of the samples presented in this work were made using scanning electron microscope FEI VERSA 3D equipped with field emission electron gun (FEG) and the energy-dispersive X-ray spectrometer (EDS) which was used for the chemical composition measurements.

The standard linear EDS analysis, in which an electron beam is moved along a single straight line, is not appropriate for analyzing the average chemical composition in the two-phase zone. In the method, the electron beam moves from one point to another and collects data from the different phases, and the grain interfaces which causes scatter of data. In this work, the

wide-line EDS method (WL-EDS) offered by TEAM™ EDS Advanced Linescan, by EDAX Software, is used to measure the concentration profiles in the diffusion zone.

In the method, the electron beam moves perpendicularly to the base line, and the data are collected from the band of a stated width covering the area on both sides of the base line, Figure 2. The collected data are averaged, and each measure point represents the averaged data collected from the rectangle $1.5 \mu\text{m}$ thick (approximate spatial resolution of EDS) and of the stated width (here $200 \mu\text{m}$).

The EDS measurements necessary to collect WL-EDS data are time-consuming. To make them more effective, without reducing quality, we have performed the optimization of the distances between electron beam tracks (the step). Three sets of data, each measured with different step sizes, 0.2, 0.6, and $1 \mu\text{m}$, were collected for $\beta|\gamma + \beta$ (β -NiAl|Ni-26Cr-17.5Al) diffusion couple subjected to 1-hour annealing at HIP conditions, 1473 K (1200 °C), 200 MPa. The obtained concentration profiles are shown in Figure 3 (left column).

It is seen that even the application of the wide-line method does not allow total elimination of data scattering in two-phase zone. The “noise” in WL-EDS is rather large. To reduce it, we have used the Savitzky–Golay filter with window $4 \mu\text{m}$.^[31] The filtered

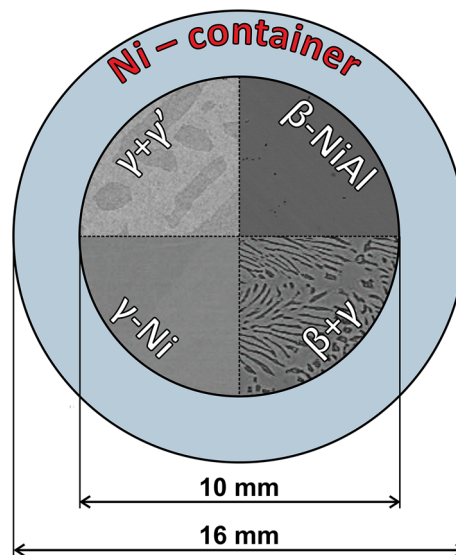


Fig. 1—A scheme of the crosssection of the studied multiple in the initial state (before annealing). The compositions of the alloys are listed in Table I.

Table I. Compositions of the Alloys Used in the Studies of the Diffusion in the Ternary Ni-Cr-Al System

Alloy Symbol: Phase Composition	Chemical Composition [At. Pct]			Manufacturer
	Ni	Cr	Al	
β	50	—	50	MaTecK
γ	100	—	—	GoodFellow
$\gamma + \gamma'$	77	5	18	
$\gamma + \beta$	56.5	26	17.5	

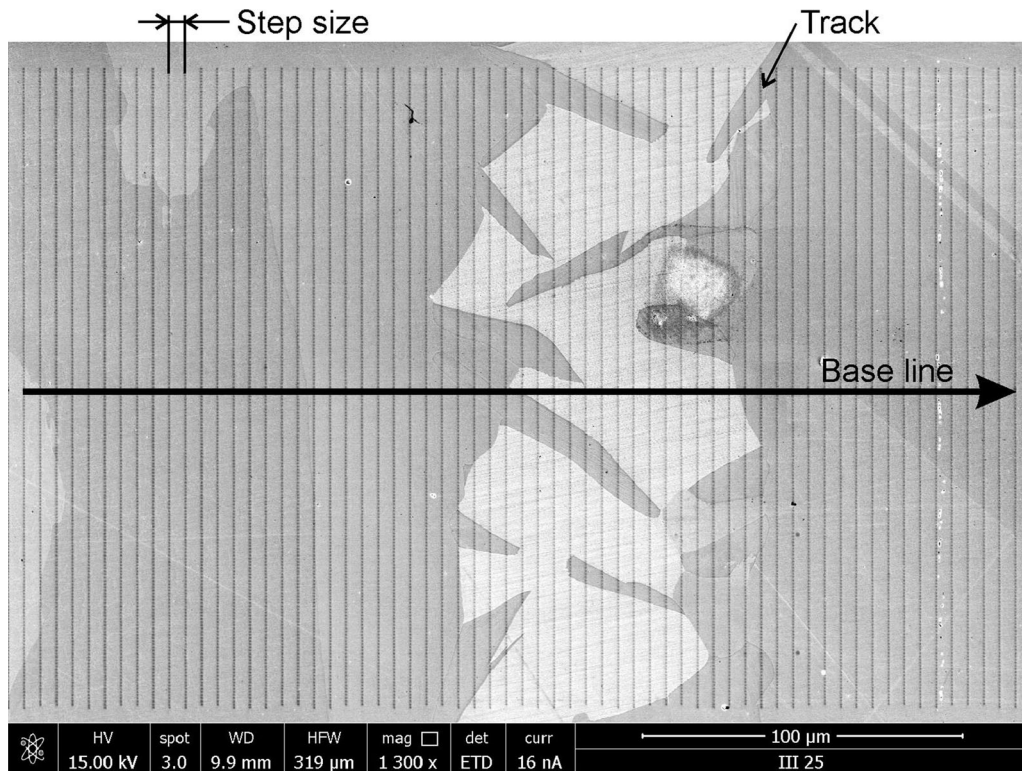


Fig. 2—A trace of the electron beam in the wide-line EDS method, recorded using the secondary electron mode. The width of the trace is $\sim 200 \mu\text{m}$ and measuring step is $5 \mu\text{m}$.

concentration profiles are presented in Figure 3 (right column).

The presented results confirm that concentration profiles are not affected by the increase of the step size from 0.2 to $1 \mu\text{m}$. The step size reduced below $1 \mu\text{m}$ ensures only small increase of the quality of the data but markedly increases the measurement time. The comparison of experimental and filtered data shows that application of Savitzky–Golay filtering significantly decreases the scattering of data. It is necessary to notice, however, that it smooths the concentration jumps at the interfaces.

Based on the obtained results, we have chosen parameters to be used for the measurements of concentration profiles in the samples annealed for 1 and 26 hours. They are $1 \mu\text{m}$ step size and $100 \mu\text{m}$ width for the samples annealed for 1 hour and $5 \mu\text{m}$ step size and $200 \mu\text{m}$ width for the samples annealed for 26 hours.

IV. MODEL AND SIMULATIONS OF THE INTERDIFFUSION

The interdiffusion model used in this work is based on the Gusk model of interdiffusion in two-phase alloys,^[37] in which it is assumed that both phases within two-phase zone are continuous and mass transport takes place in both them. Similar model, but in the reduced form (assumed diffusion through one phase only), is extensively used by Morral *et al.*^[38]

In this work, we study interdiffusion in the one-dimensional multiphase ternary Ni-Cr-Al couple. We

assume that the diffusion couple forms a closed ternary system and diffusion occurs through all phases at constant temperature.^[32,39] There can coexist two phases within a single layer and the sum of their fractions is 1. Local ortho-equilibrium between the phases is assumed. To generalize the model, we allow various partial molar volumes of the components in the phases, Ω_i^j , and various partial molar volumes of the phases, Ω^j . In the model, the unknowns are concentrations (c_{Ni}, c_{Cr}, c_{Al}), drift velocity, the same for all components, due to interdiffusion within the phases (v^j), drift velocity due to the different partial molar volumes of the phases (γ, γ' and β), v , and volume fractions of the phases, φ^j .

The unknowns are calculated by solving the set of equations

By mass conservation law,

$$\frac{\partial c_i}{\partial t} = -\frac{\partial}{\partial x} \left(\varphi \tilde{J}_i^\alpha + (1 - \varphi) \tilde{J}_i^\beta + c_i v \right) \text{ for } i = 1, 2, 3, \quad [1]$$

where $\varphi = \varphi^\alpha$ and $1 - \varphi = \varphi^\beta$;

Volume continuity equations:

$$\frac{\partial}{\partial x} \left(\sum_i \Omega_i^j D_i^j \nabla c_i^j - v^j \right) = 0 \text{ for } j = \alpha, \beta, \quad [2]$$

$$\frac{\partial v}{\partial x} = -\frac{\Omega^\alpha - \Omega^\beta}{3\Omega} \frac{\partial \varphi}{\partial t}, \quad [3]$$

where Ω is a local molar volume of two-phase alloy;

By Lever rule,

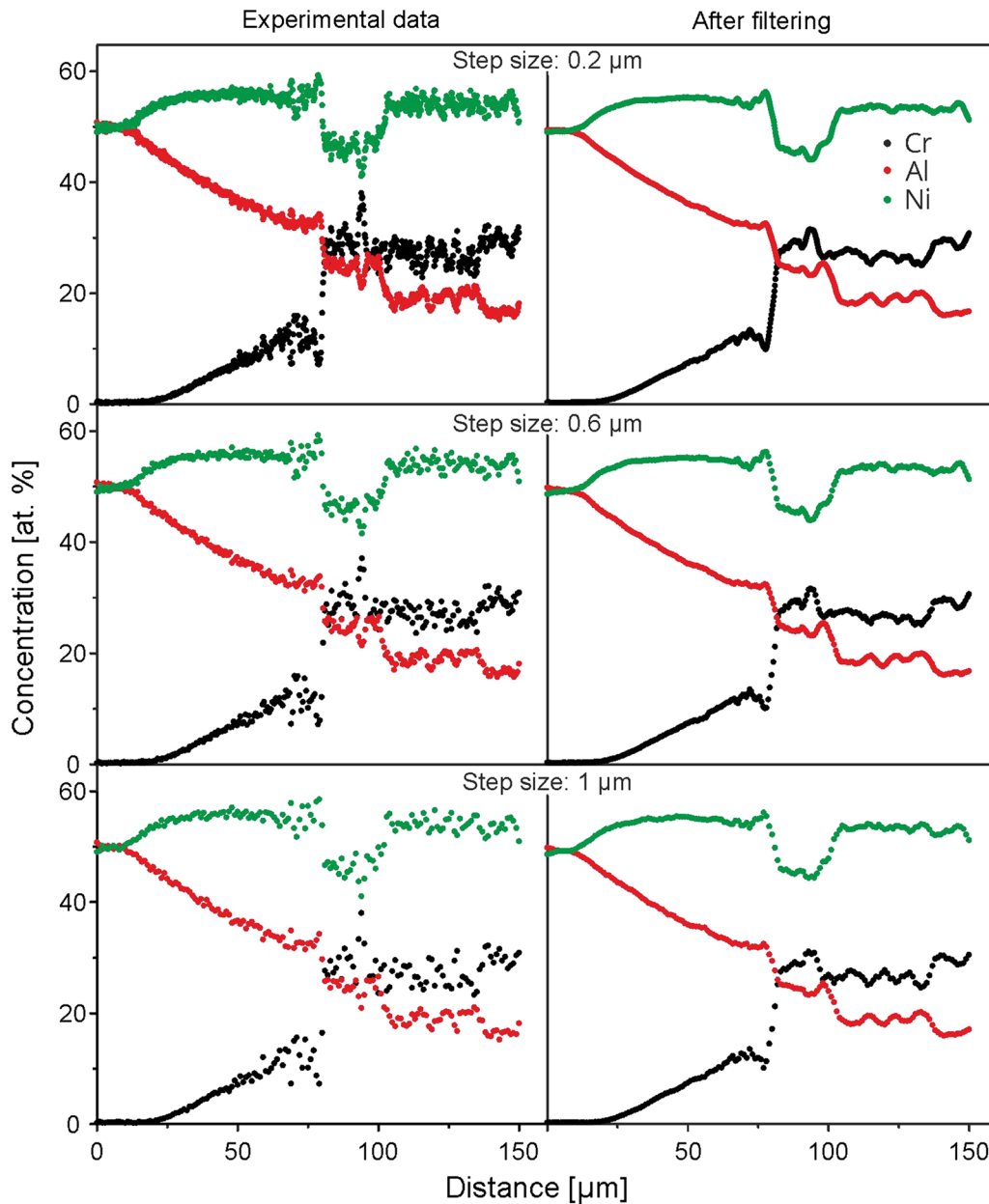


Fig. 3—Concentration profiles in the $\beta/\gamma + \beta$ (β -NiAl|Ni26Cr17.5Al) diffusion couple after 1-h annealing at HIP conditions, 1473 K (1200 °C), 200 MPa. Comparison of the profiles measured by WL-EDS technique at different step sizes, from the top: 0.2, 0.6, and 1 μm , before (left column) and after filtering by Savitzky-Golay filter with the window 4 μm (right column).

$$\varphi = \frac{c_i - c_i^\beta}{c_i^\alpha - c_i^\beta} \quad [4]$$

The interdiffusion flux in each phase is given by the bi-velocity formalism:

$$\tilde{J}_i^j = -D_i^j \nabla c_i^j + c_i^j v^j, j = \alpha, \beta, i = 1, 2, 3. \quad [5]$$

In calculations and presentation of data (diffusion paths), we have used phase diagram after Dupin *et al.*^[19] and for simplification assumed that all tie lines in $\alpha + \beta$ zone are distributed radially so they cross in one point.

Details of the model and method of calculations of the equilibrium concentrations in phases are presented in Reference 32.

First we made some test calculations aimed to compare the present model with the results previously obtained within DICTRA.^[40] The calculations were made for two-phase diffusion couple with the boundary “0” type $\alpha + \beta$ ($\alpha + \beta$ (Ni20Cr19.5Al|Ni15.5Cr22Al), at 1473 K (1200 °C). The results are shown in Figure 4 and confirmed good agreement between the sets of data. The main differences are due to differences in phase diagram, strictly due to assumption about radial distribution of the tie lines.

As the agreement is good, it has prompted us to simulate interdiffusion in the diffusion couples like in the

experiment, Table I. Simulations were made for the $\gamma + \gamma'$ and $\gamma + \beta$ alloys (Table I) coupled with γ single-phase Ni.

It has been assumed that the samples were annealed for 1 and 26 hours at 1473 K (1200 °C) as in the experiment. To accelerate the computing speed, the evolutionary time step was assumed. The chosen widths of the diffusion couple were, respectively, 300 μm for 1-hour annealing and 1600 μm for 26-hours annealing, 200 and 400 grid points which were taken in calculations, respectively. The polynomials describing phase boundaries and the points of intersection of the tie lines for equilibrium of the phases in $\beta + \gamma$ and $\gamma + \gamma'$ fields have been calculated based on the phase diagram by Dupin *et al.*^[19] and are shown in Table II.

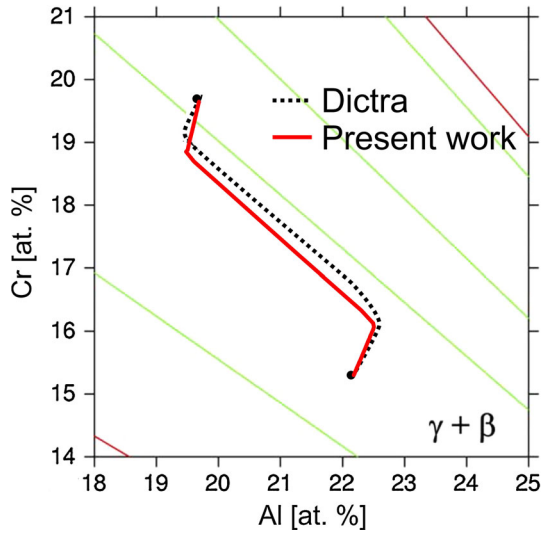


Fig. 4—A comparison of diffusion paths in $\gamma + \beta | \gamma + \beta$ (Ni20-Cr19.5Al|Ni15.5Cr22Al) and diffusion couples, 1473 K (1200 °C), calculated according to the present model and within DICTRA. DICTRA data applied after.^[40]

To choose the interdiffusion coefficients, we considered the works by Nesbitt^[27] and Mehrer^[41] who showed that the chromium cross diffusion coefficient, \tilde{D}_{CrAl}^{Ni} , decreases significantly when the chromium concentration is lower than ~25 pct. Otherwise, Chen^[42] showed that the diffusivities in $\gamma + \beta$ phase zone do not radically change due to the composition changes and that the influence of the variation of the diffusivities on the diffusion path is negligible. In the present simulations, we have used average diffusivities calculated from Thermocalc database, for the γ -phase presented by Chen and Zhao^[40,42] and for the β -phase presented by Campbell,^[44] Table III. In the same table, the partial molar volumes for all phases are presented. The partial molar volumes of the components in γ' and β phases are assumed the same for each component. For γ -phase, they differ.^[43]

V. RESULTS

SEM images of the multiples, shown in Figure 5, confirm that the applied procedure allows obtaining good connection between the alloys. Even in the central part of the diffusion multiple, the diffusion zone has been formed. Only small deformation of the alloys can be seen, which is due to differences in their mechanical and thermal properties.

Elemental analysis confirms, that neither aluminum nor chromium oxides, have been formed. For better imaging of the interdiffusion in the multiple, 2D concentration maps were drawn, Figure 5(b) through (d). They cover central joins of all alloys, the area 300 \times 270 μm . It is seen that some of the isoconcentration lines overlap with the boundaries visible in SEM images and that the range of 2D diffusion zone does not exceed 100 μm . Accordingly, 2D diffusion in the center does not affect the quasi one-dimensional diffusion zone analyzed here. Observed irregular shape of isoconcentration lines and the loops are due to a character of two-phase microstructure of the alloy, especially $\gamma + \beta$ region.

Table II. Phase Boundaries Relations and Common Tie-Lines Points, \mathbf{p}^{tie} , Used to Calculate Local Equilibrium in the Two-Phase Zones^[19]

Phase Boundary	Relation	Common Tie-Lines point: \mathbf{p}^{tie}
$\beta \beta + \gamma$	$k^{\beta}:N_2 = 0.2216N_1 + 0.2752$	(-0.0077, 0.4195)
$\gamma \beta + \gamma$	$k^{\gamma}:N_2 = -0.2264N_1 + 0.2003$	
$\gamma' \gamma + \gamma'$	$k^{\gamma'}:N_2 = 8.2533(N_1)^2 - 0.7857N_1 + 0.2323$	(0, 0.2793)
$\gamma \gamma + \gamma'$	$k^{\gamma}:N_2 = 2.0422(N_1)^2 - 0.4041N_1 + 0.1845$	

Table III. Diffusion Coefficients, D_i^j , and Partial Molar Volumes, Ω_i^j , in β , γ' , and γ Phases at 1473 K (1200 °C)^[40,42-44]

	Component, i , Phase, j	Ni	Cr	Al
Diffusion Coefficient [cm^2/s]	β	1.2×10^{-9}	1.2×10^{-9}	1.4×10^{-9}
	γ'	3.2×10^{-11}	1.2×10^{-10}	1.0×10^{-10}
	γ	3.2×10^{-10}	2.6×10^{-9}	1.1×10^{-9}
Partial Molar Volume [cm^3/mol]	γ	7.2	10.0	6.6
	β	8.3	8.3	8.3
	γ'	7.4	7.4	7.4

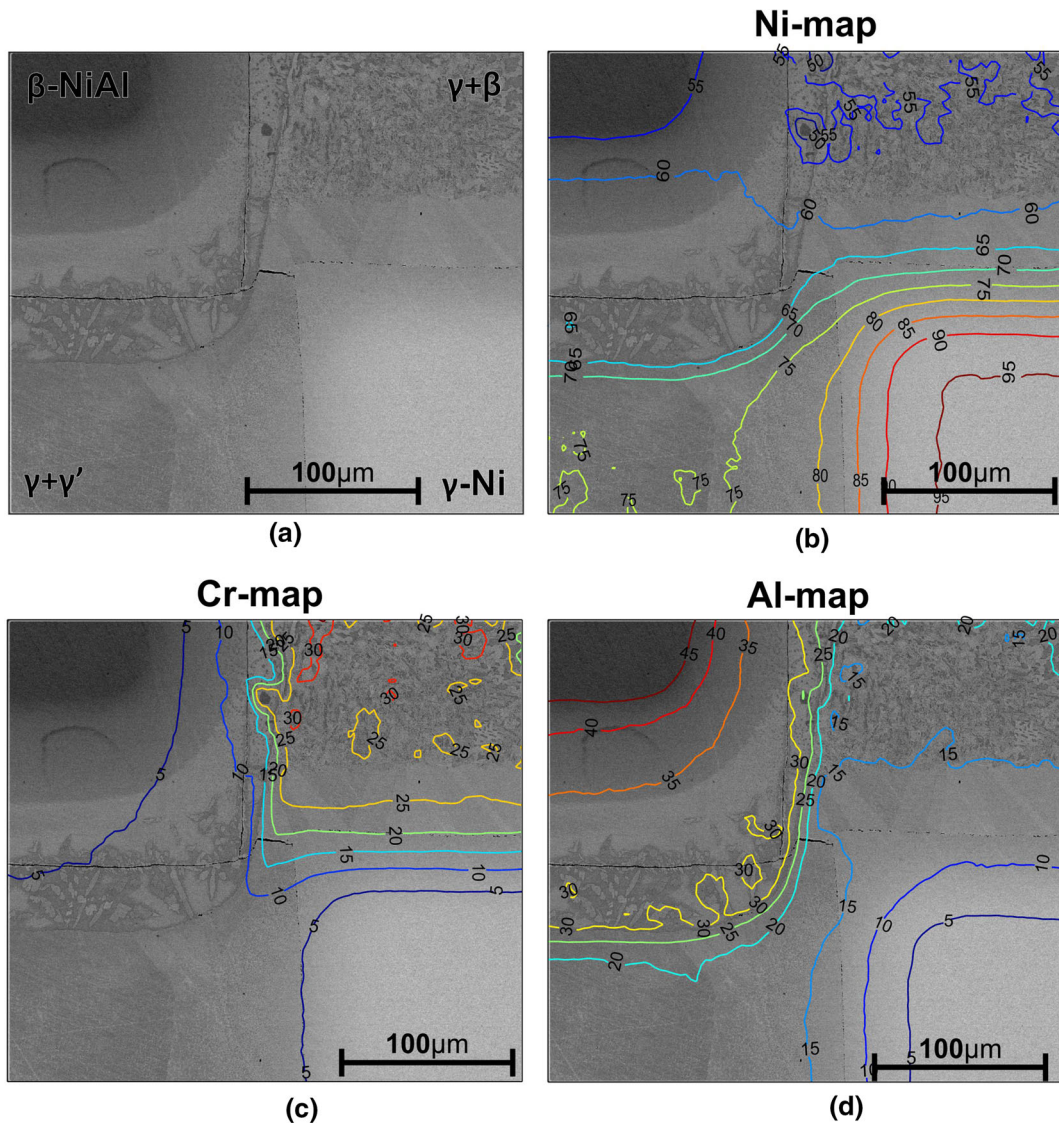


Fig. 5—Isoconcentration 2D maps for the central area of the multiple, annealed at 1473K (1200 °C) for 1 h: (a) SEM image of central area, (b) nickel map, (c) chromium map, (d) aluminum map.

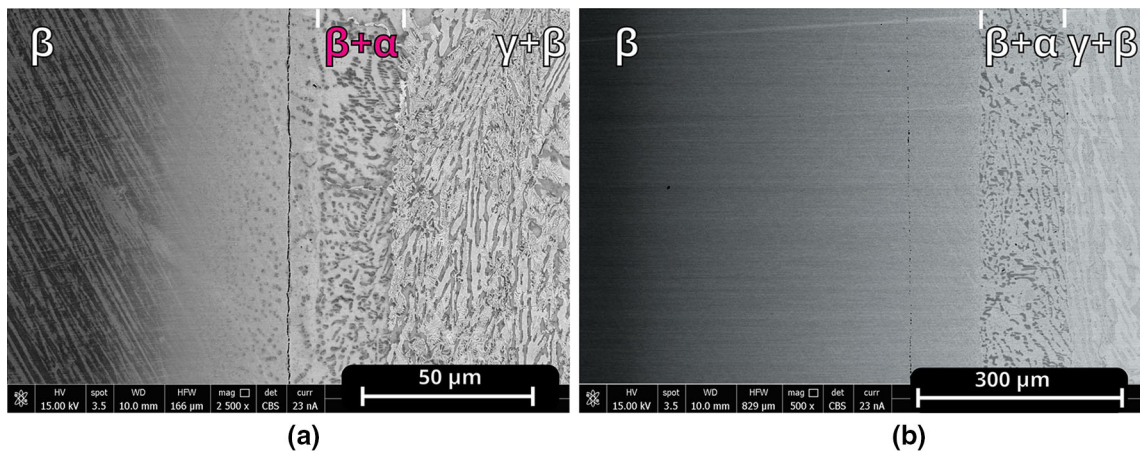


Fig. 6—SEM image of the $\beta(\gamma + \beta)$ and β -NiAl/Ni26Cr17.5Al of diffusion couple subjected to annealing at 1473 K (1200 °C) for (a) 1 h; (b) 26 h.

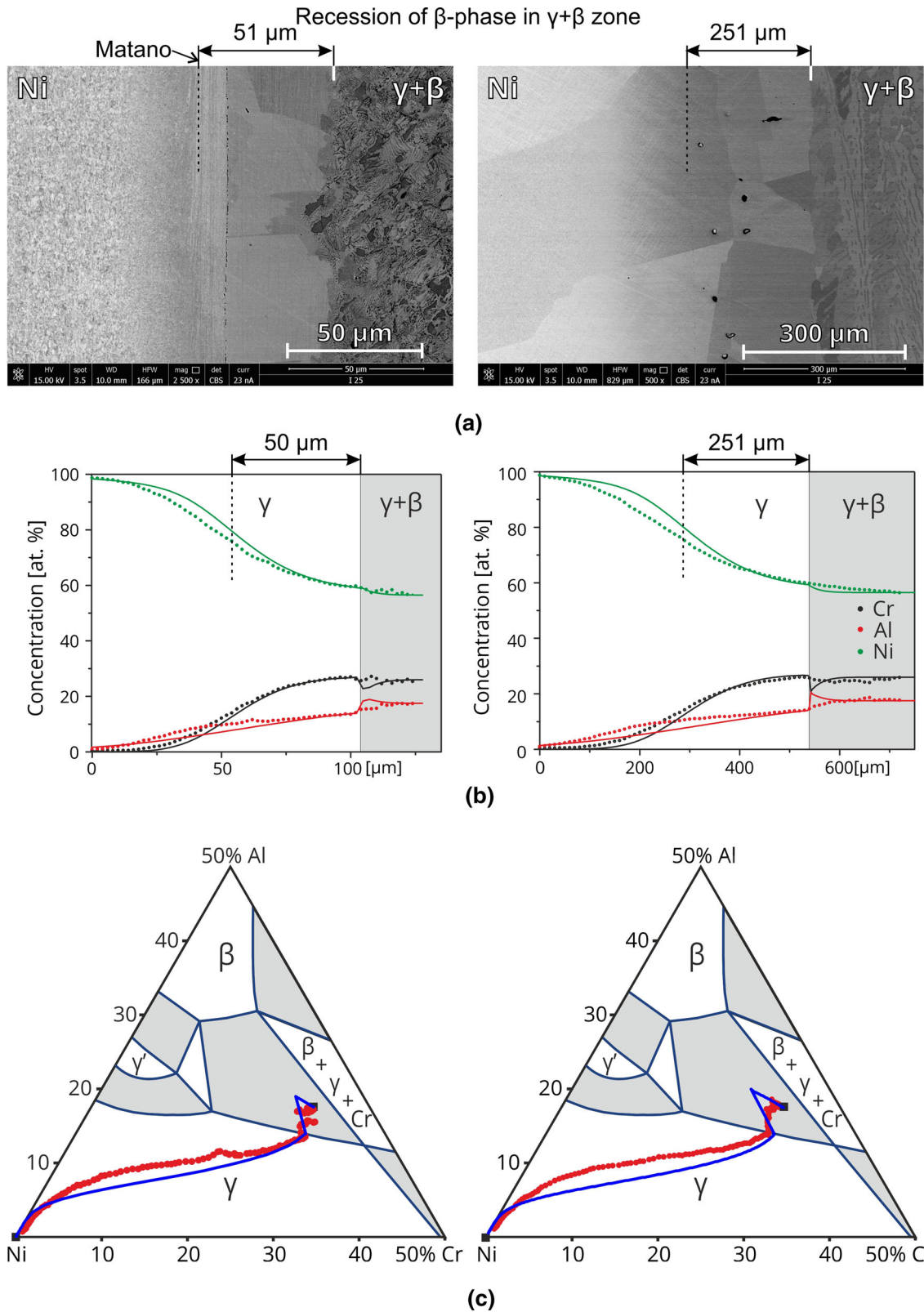


Fig. 7—Interdiffusion in $\gamma/(\gamma + \beta)$ and Ni/Ni₂₆Cr_{17.5}Al of diffusion couple subjected to annealing at 1473 K (1200 °C) for 1 (left) and 26 h (right). (a) SEM images, Matano planes, interphase boundaries and the recession of β phase are indicated; (b) experimental (dots) and simulated (solid lines) concentration profiles; (c) experimental (dots) and simulated (solid line) diffusion paths between terminal alloys (black squares); gray areas are two-phase fields.

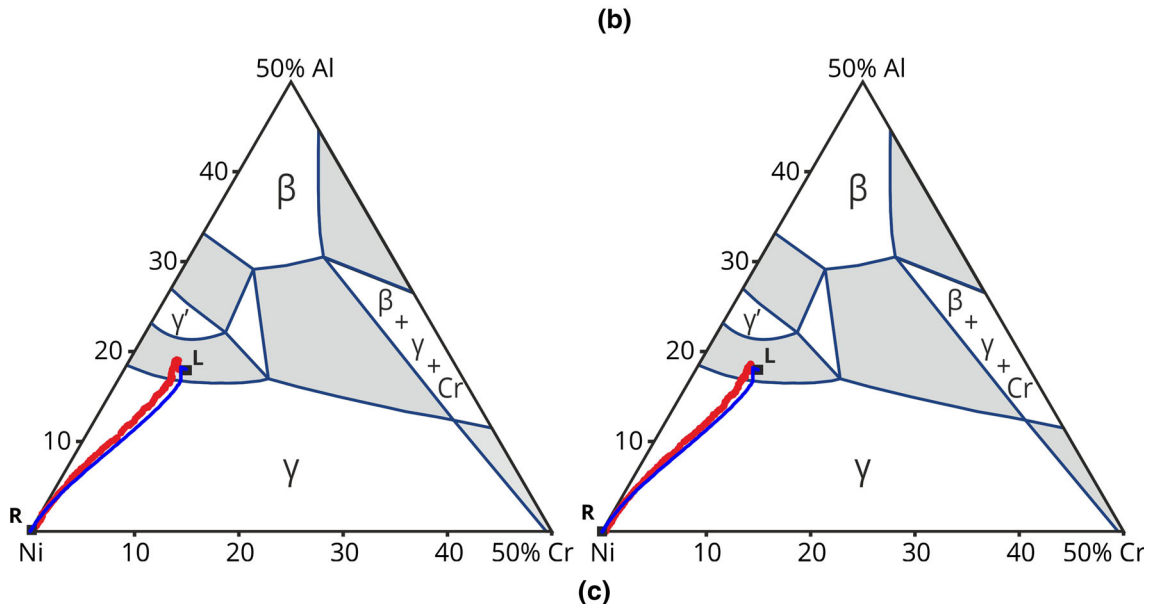
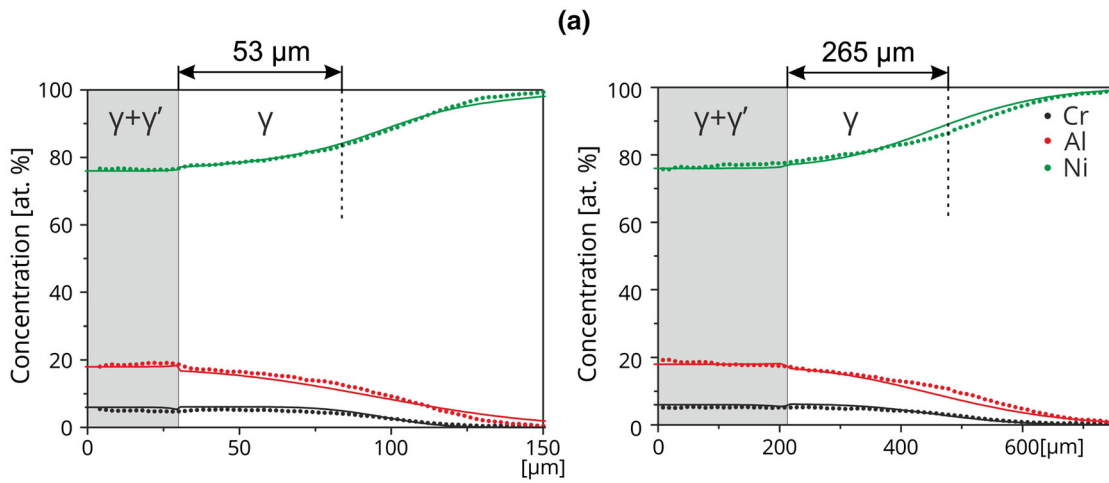
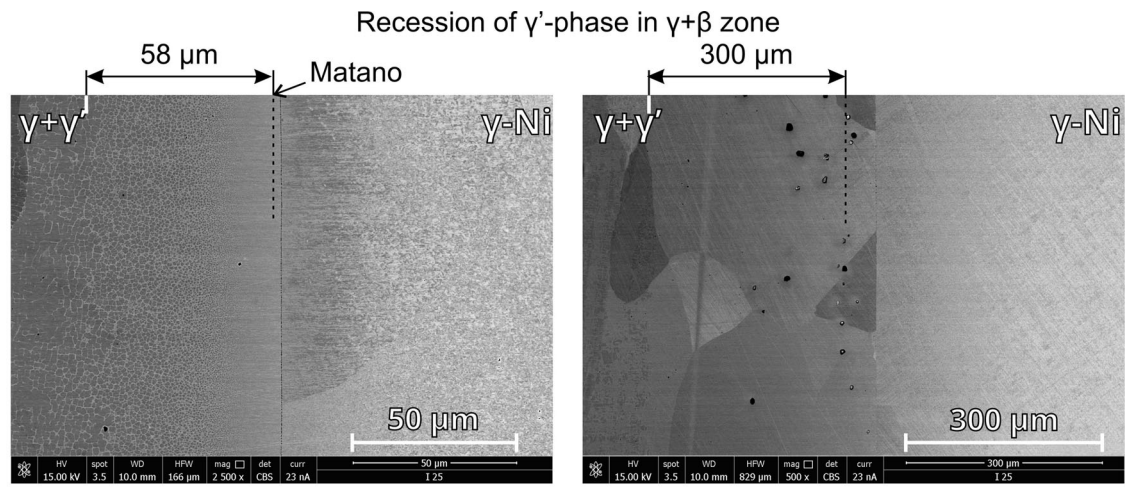


Fig. 8—Interdiffusion in $(\gamma + \gamma')/\gamma$ and Ni5Cr18Al|Ni of diffusion couple subjected to annealing at 1473 K (1200 °C) for 1 (left) and 26 h (right). (a) SEM images, Matano planes, interphase boundaries, and the recession γ' -phase are indicated; (b) experimental (dots) and simulated (solid lines) concentration profiles; (c) experimental (dots) and simulated (solid line) diffusion paths between terminal alloys (black squares); gray areas are two-phase fields.

The SEM images of the diffusion zone in the $\beta|(\gamma + \beta)$ and β -NiAl|Ni₂₆Cr_{17.5}Al of diffusion couple subjected to 1- and 26-hour annealing are shown in Figure 6. The concentration profiles corresponding to the interdiffusion in the sample subjected to 1-hour annealing are shown in Figure 3.

The microstructure images reveal that in both samples the $\alpha + \beta$ two-phase layers have grown between the β single-phase and the $\gamma + \beta$ two-phase layers. Apparently, the diffusion path passes through the $\alpha + \beta$ two-phase region.

The results obtained for $\gamma|\gamma + \beta$ and $\gamma + \gamma'|\gamma$ couples are shown in Figures 7 and 8, respectively. We show the SEM images, concentration profiles, and diffusion paths for the samples annealed for 1 (left) and 26 hours (right). Next to the experimental concentration profiles and diffusion paths, the simulated data are presented.

The results for all couples are similar. In the SEM image, a characteristic recessions of β -phase in $\gamma + \beta$ zone and γ' -phase in $\gamma + \gamma'$ zone are seen. It is measured as a shift of the type 1 interphase boundary from the initial position (Matano plane). A diffusion paths within the γ single-phase region assume typical S-shape, while within the $\gamma + \beta$ and the $\gamma + \gamma'$ two-phase regions, they have zigzag shapes, Figures 7 and 8. The zigzag in $\gamma + \gamma'$ region is not observed which is probably due to the low-spatial resolution of WL-EDS. Visible differences in the microstructures of the samples annealed by 1 and 26 hours are because of different cooling conditions.

For all couples, a very good agreement of the computed and experimentally measured position of the type 1 interphase boundary was achieved. Also good agreement was obtained between the calculated and measured diffusion paths and concentration profiles for interdiffusion in the γ -phase. The simulated results show, however, larger jump of the concentration than the measured data. One can associate this difference to three various sources:

- Experimental “smoothing” due to increased step applied in the WL-EDS measurements and application of filtering procedure;
- Application of the constant diffusion coefficients, concentration independent;
- Application of the Fickian flux formula appropriate for ideal systems instead of application of the gradient of chemical potential which is the true driving force in non-ideal Ni-Cr-Al system.

VI. SUMMARY

Studies of interdiffusion in multicomponent–multiphase systems present a difficult task. In this work, we have presented the results of joined experimental and numerical studies of interdiffusion in Ni-Cr-Al ternary alloys. The diffusion couples were made by applying the multi-couple method followed by HIP procedure combined with annealing in vacuum-closed ampoule. The applied method allowed obtaining high-quality, planar, repetitive, and oxide-free diffusion couples.

In the measurements of the concentration profiles, the WL-EDS technique has been applied for the first time. It is shown that the method is very reliable in the measurements of average concentrations within multiphase alloys. For better effectiveness and making a method less time-consuming, we have applied data filtering. Experimental studies have been followed by numerical simulations performed by multicomponent–multiphase interdiffusion model based on Gusak model coupled with Darken formalism.^[30,32,37,45] In contrast to earlier simulations by Morral *et al.*,^[38,40,42] the diffusion through both phases is assumed in the present calculations. The results, concentration profiles and diffusion paths, show good agreement with experimental data.

Such consistent studies which present fusion of experiment with numerical simulations of interdiffusion in Ni-Cr-Al $\gamma + \gamma'$, $\gamma + \beta$, and $\alpha + \beta$ alloys are presented for the first time. Good agreement between experimental and simulated data confirms that the proposed model based on Darken formalism can be successfully applied to study mass transport in multicomponent–multiphase alloys. The reliability of WL-EDS technique is also confirmed.

ACKNOWLEDGMENTS

This work is supported by a National Science Center (Poland) decision DEC-011/02/A/ST8/00280.

OPEN ACCESS

This article is distributed under the terms of the Creative Commons Attribution 4.0 International License (<http://creativecommons.org/licenses/by/4.0/>), which permits unrestricted use, distribution, and reproduction in any medium, provided you give appropriate credit to the original author(s) and the source, provide a link to the Creative Commons license, and indicate if changes were made.

REFERENCES

1. A. Engstrom, J.E. Morral, and J. Agren: *Acta Mater.*, 1997, vol. 45, pp. 1189–99.
2. I. Kaur, Y. Mishin, and W. Gust: *Fundamentals of Grain and Interphase Boundary Diffusion*, Wiley, Chichester, 1995.
3. R.C. Reed: *The Superalloys: Fundamentals and Applications*, Cambridge University Press, Cambridge, 2006.
4. A. Taylor and R.W. Floyd: *J. Inst. Met.*, 1952, vol. 81, pp. 451–64.
5. I.I. Kornilov and R.S. Mints: *Izv. Sekts Fiz.-Khim. Anal.*, 1953, vol. 22, pp. 111–16.
6. A. Yu: *Bagaryatskiy. Russ. J. Inorg. Chem.*, 1958, vol. 3, pp. 247–52.
7. D.C. Tu and L.L. Seigle: *Thin Solid Films*, 1982, vol. 95, pp. 47–56.
8. S. Ochiai, Y. Oya and T. Suzuki: *Bull. Res. Lab. Precis. Mach. Electron.*, 1983, pp. 1–17.
9. S.M. Merchant and M.R. Notis: *Mater. Sci. Eng.*, 1984, vol. 66, pp. 47–60.
10. Y.M. Hong, H. Nakajima, Y. Mishima, and T. Suzuki: *ISIJ Int.*, 1989, vol. 29, pp. 78–84.

11. P. Rogl: *Ternary Alloys: Comprehensive Compendium of Evaluated Constitutional Data and Phase Diagrams*, VCH Publishers, Weinheim, 1991.
12. C.C. Jia, K. Ishida, and T. Nishizawa: *Metall. Mater. Trans. A*, 1994, vol. 25, pp. 473–85.
13. E. Rosell-Laclau, M. Durand-Charre, and M. Audier: *J. Alloys Comp.*, 1996, vol. 233, pp. 46–263.
14. D. Tu: Ph. D. Dissertation, State University of New York at Stony Brook, 1982.
15. R.F. Decker: *Strengthening Mechanisms in Nickel-Base Superalloys*, International Nickel, New York, 1969.
16. I. Ansara, N. Dupin, H.L. Lukas, and B. Sundman: *J. Alloys Comp.*, 1997, vol. 247, pp. 20–30.
17. W. Huang and Y.A. Chang: *Intermetallics*, 1998, vol. 6, pp. 487–98.
18. W. Huang and Y.A. Chang: *Intermetallics*, 1999, vol. 7, pp. 863–74.
19. N. Dupin, I. Ansara, and B. Sundman: *Calphad*, 2001, vol. 25, pp. 279–98.
20. S.R. Le Vine: *Metall. Mater. Trans. A*, 1978, vol. 9, pp. 1237–50.
21. L.A. Carol: *A Study of Interdiffusion in $\beta + \gamma + \gamma'$ Ni-Cr-Al Alloys at 1200 °C*, Michigan Technological University, Houghton, 1985.
22. J.A. Nesbitt and R.W. Heckel: *Metall. Trans. A*, 1987, vol. 18A, pp. 2087–94.
23. S.M. Merchant, M.R. Notis, and J.I. Goldstein: *Metall. Trans. A*, 1990, vol. 21, pp. 1901–10.
24. S.M. Merchant, M.R. Notis, and J.I. Goldstein: *Metall. Trans. A*, 1990, vol. 21, pp. 1911–19.
25. X. Qiao: University of Connecticut, 1998.
26. J.A. Nesbitt and R.W. Heckel: *Metall. Trans. A*, 1987, vol. 18A, pp. 2061–73.
27. J.A. Nesbitt and R.W. Heckel: *Metall. Trans. A*, 1987, vol. 18A, pp. 2075–86.
28. K. Wu, Y.A. Chang, and Y. Wang: *Scr. Mater.*, 2004, vol. 50, pp. 1145–50.
29. J.-C. Zhao: *J. Mater. Res.*, 2001, vol. 16, p. 1565.
30. M. Zajusz: Ph.D. Thesis, AGH University of Science and Technology, 2016.
31. A. Savitzky and M.J.E. Golay: *Anal. Chem.*, 1964, vol. 36, pp. 1627–39.
32. M. Zajusz, B. Bożek, K. Tkacz-Śmiech, K. Berent, and M. Danielewski: *Defect Diffus. Forum*, 2016, vol. 369, pp. 77–82.
33. J.-C. Zhao: *Adv. Eng. Mater.*, 2001, vol. 3, p. 143.
34. J.-C. Zhao, M.R. Jackson, and L.A. Peluso: *Acta Mater.*, 2003, vol. 51, pp. 6395–6405.
35. C.E. Campbell, J.-C. Zhao, and M.F. Henry: *Mater. Sci. Eng. A*, 2005, vol. 407, pp. 135–46.
36. J.-C. Zhao: *Prog. Mater. Sci.*, 2006, vol. 174, pp. 557–631.
37. A.M. Gusak and Y.A. Lyashenko: *J. Eng. Phys.*, 1991, vol. 59, pp. 1044–49.
38. W.D. Hopfe and J.E. Morral: *Acta Metall. Mater.*, 1994, vol. 42, pp. 3887–94.
39. M. Danielewski, R. Filipek, K. Holly, and B. Bożek: *Phys. Status Solidi A*, 1994, vol. 145, pp. 339–50.
40. H. Yang, J.E. Morral, and Y. Wang: *Acta Mater.*, 2005, vol. 53, pp. 3775–81.
41. H. Mehrer: *Diffusion in Solids*, Springer, Berlin Heidelberg, 2007.
42. H. Chen and J.E. Morral: *Acta Mater.*, 1999, vol. 47, pp. 1175–80.
43. R.L. David: *CRC Handbook of Chemistry and Physics*, CRC Press, Boca Raton, 2005.
44. C.E. Campbell: *Acta Mater.*, 2008, vol. 56, pp. 4277–90.
45. L.S. Darken: *Trans. AIME*, 1948, vol. 175, pp. 184–201.